Received: 30 March 2020 | Revised: 4 August 2020 | Accepted: 25 August 2020

DOI: 10.1111/str.12370

FULL PAPER

strain WILEY

Towards Material Testing 2.0. A review of test design for identification of constitutive parameters from full-field measurements

F. Pierron[1] | M. Grédiac[2]

[1]Faculty of Engineering and Physical Sciences, University of Southampton, Southampton, UK

[2]Institut Pascal, UMR CNRS 6602 BP 10448, Université Clermont Auvergne, Clermont-Ferrand, France

Correspondence
F. Pierron, Faculty of Engineering and Physical Sciences, University of Southampton, University Road, Southampton SO17 BJ, UK.
Email: f.pierron@soton.ac.uk

Abstract

Full-field optical measurements like digital image correlation or the grid method have brought a paradigm shift in the experimental mechanics community. While inverse identification techniques like finite element model updating or the virtual fields method have been the object of significant developments, current test methods, inherited from the age of strain gauges or linear variable displacement transducers, are generally not well adapted to the rich information provided by these new measurement tools. This paper provides a review of the research dealing with the design and optimization of heterogeneous mechanical tests for the identification of material parameters from full-field measurements, christened here Material Testing 2.0 (MT2.0).

KEYWORDS

finite element model updating, full-field measurements, inverse identification, MT2.0, optimization, test design, virtual fields method

1 | INTRODUCTION

Full-field measurement techniques such as digital image correlation (DIC[1]) or the grid method (GM[2]) have become mature and are now widespread in the experimental mechanics community. This is mainly due to the fact that these techniques are able to provide, within certain limits, displacement and strain fields that occur at the surface of specimens of various shapes subjected to thermomechanical loadings. In a context of material characterization, such measurements make it possible to move from simple statically determinate tests to more complex ones, with a view to get more data from a single test, thus reducing the testing effort and increasing the quality of the material models. It should be noted that for mesoscopically heterogeneous materials such as welds, large weave composites or graded foams, the traditional test methods only provide an averaged behaviour while full-field measurement have the potential to identify spatially varying properties.

The problem with this approach however is that in general, no closed-form expression linking local kinematic measurements to constitutive parameters is available. Therefore, early research focused on developing robust and efficient techniques to identify material parameters from full-field measurements in that case. The need for optimizing test configurations adapted to this new paradigm emerged later, as the breadth of applications increased.

Using more complex tests, full-field measurements and inverse identification to identify mechanical constitutive parameters is a new paradigm in material testing that for the moment has been confined to research laboratories. There

is no doubt that in the coming years, such approaches will develop further and will eventually lead to new test methods widely adopted by both academia and industry. For the sake of providing visibility to this technical area, the authors of this paper feel that a new denomination has to be introduced. It is proposed to refer to this as 'Material Testing 2.0' (MT2.0), capturing the fact that this will lead to a complete revamp of mechanical tests, eventually leading to new standards as cameras gradually replace strain gauges and extensometers in testing laboratories. This denomination, MT2.0, will be used in the rest of the paper for the sake of clarity and brevity.

The objective of this paper is to propose a review of the research dealing with the design and optimization of mechanical tests dedicated to MT2.0.

It is worth noting that optimizing test configurations has been a research topic for a long time. However, with the classical approach of mechanical testing, which solely uses a limited number of isolated sensors, the focus has generally been on optimizing the placement and orientation of the sensors to collect the most relevant information. Optimal placement of strain gauges,[3,4] accelerometers[5-7] or even GPS sensors on wide structures like bridges[8] has been addressed in the literature. The proposed methodologies generally rely on statistical properties that have to be satisfied.[9] They are of general purpose and can be employed in other fields than experimental mechanics.[10-12] However, since full-field measurements provide spatially dense data, such methods devised for a small number of data points are generally irrelevant. The best placement of cameras for 3D measurements or the best location of displacement sensors still represents an open problem when full-field measurements are employed or when constitutive parameters are identified by inverse analysis, Vitse et al.[13] and Huang et al.,[14] respectively. But the present review will focus exclusively on designing specific specimen geometry and loading configuration for the identification of constitutive parameters from either displacement or strain fields.

In this review, the papers have been classified according to four different categories following a progression of sophistication:

- Design by intuition
- Design by strain state
- Design by identification quality
- Design by full identification simulation

The first level, 'design by intuition', consists in devising test configurations arbitrarily based on previous experience or intuition. However, as the complexity of the models increases, together with the number of parameters to be identified, this approach generally leads to considerably sub-optimal configurations and more rational approaches to test design have to be proposed. A natural idea, referred to here as 'design by strain state', is to use the strain state as a design variable, as this bears witness of the material parameters. By trying to balance the different components, one can hope to improve identifiability. However, the dependence of the sought parameters to the strain components can be complex, and a more relevant approach, called here 'design by identification quality', consists in using the quality of the identification as an optimization criterion, generally using kinematic data directly from numerical simulations. Nevertheless, this does not take into account important features coming from the measurements themselves, including hardware performance and image processing parameters. Therefore, the most sophisticated approach to date, 'design by full identification simulation', consists in simulating the whole identification chain, from image formation all the way to identification. This allows for full uncertainty propagation to be captured and for more realistic identification performance to be derived, which can then be used for test design and optimization.

The present paper is organized as follows. First, the two main identification techniques currently in use are briefly reviewed, namely, finite element model updating (FEMU) and the virtual fields method (VFM). Then, representative articles in the four different categories of tests mentioned above are presented and discussed in separated sections. Some perspectives and recommendations are finally offered.

2 | MAIN PROCEDURES USED TO EXTRACT CONSTITUTIVE PARAMETERS FROM FULL-FIELD MEASUREMENTS

Before designing MT2.0 tests, the first step has been to elaborate procedures that could be used to extract constitutive parameters from heterogeneous strain fields, in cases for which no closed-form expression exists between these

unknown parameters and the local deformation measurements. FEMU and the VFM have progressively imposed themselves as the two main techniques for this. The main features of both methods are briefly recalled hereafter.

2.1 | Finite element model updating

To the best of the authors' knowledge, the idea of updating a finite element model in order to identify material properties has been given for the first time in the early 70s in Kavanagh and Clough,[15] in the case of linear and non-linear elasticity. Updating is performed by minimizing a cost function with respect to the sought parameters, this cost function reflecting the 'distance' between displacements measured at some points, and their counterparts estimated with FE computation at a given iteration. A cross-shaped specimen subjected to two perpendicular loads was used to this end in this reference. At that time, optimizing the test configuration was not the objective, but the underpinning idea was that the location of the applied load and the geometry of the specimen would be such that its response was 'sufficiently' influenced by all the unknowns, so that they could be identified. A hole was added in order to increase heterogeneity. It is worth noting that FEMU does not necessarily require full-field measurements. Only numerical simulations were presented in Kavanagh and Clough,[15] but this paper served as a starting point to many subsequent studies where this idea was employed with actual measurements. For instance, shortly after this first reference, its first author used input data provided by a limited number of strain gauges.[16] It seems that Courtade et al.[17] is the first example where FEMU input data are full-field measurements. Composite materials were tested in this reference. This was the starting point of many developments covering various materials and types of constitutive equations. Examples dealing with biological materials,[18,19]metals,[20-25] MEMS,[26] composites,[27-30] heterogeneous[31] and homogeneous[32] hyperelastic materials, wood,[33] and even crimped mineral wool,[34] can be found in the literature. Note finally that when DIC is the measuring technique, it is possible to merge the two steps involved in the procedure described above, namely, measuring the displacement field on the one hand, and then applying FEMU on the other hand. This leads to the so-called integrated DIC (IDIC) introduced in Mathieu et al.[24] In this reference, the authors find that merging or not these two steps gives equivalent results, while Ruybalid et al.[25] claims the integrated version leads to more reliable results. It seems however that this approach has not yet been widely used, so we consider here that IDIC is a particular case of FEMU coupled with DIC measurements.

The main strength of FEMU is that it relies on the finite element method, which is a versatile tool widely used in the solid mechanics community. This is also its main weakness. Indeed, FE was initially developed for a different problem, namely, finding the displacement/strain/stress fields by assuming that the constitutive equations and their governing parameters are known. Using this tool to solve the material identification problem automatically leads the identification procedure to be iterative, even in the simplest case of linear elasticity. As a consequence, FEMU is generally quite computationally intensive, particularly for geometrical or material non-linearities. Finally, boundary conditions are necessary to perform any FE calculation, and feeding FEMU with faithful experimental boundary conditions is often challenging, especially in terms of force distributions. DIC-measured displacements at the boundary of the field of view can be used, but their noisy nature also creates specific problems.

2.2 | The VFM

The drawbacks of FEMU have led researchers to elaborate alternative procedures which could straightforwardly (instead of iteratively) provide the unknown parameters. In this regard, a pioneering approach was proposed in 1986 in Foudjet.[35] It consisted in using the Maxwell-Betti reciprocal work theorem in order to identify the six independent bending stiffnesses of wood plates. Indeed, assuming linear elasticity for the constitutive materials, considering a simple square plate subjected to three different loads and mixing the three corresponding deflection fields leads to six independent equations since the work done by the forces applied in test #i through the displacement of test #j is equal to the work done by the forces applied in test #j through the displacement of test #i. The system formed by these six equations being linear, the six unknowns are found after a mere inversion. The drawback is that even if only one specimen is sufficient to identify six independent parameters with this approach, three different tests must be performed on the same specimen to obtain a set of independent equations. Another point is that measurements are always noisy, and two measurement fields are involved in each equation, which makes this approach rather noise-sensitive.

These two limitations (i. three different tests and ii. results highly sensitive to noise) have led a related approach to emerge in Grédiac[36] and Grédiac and Vautrin.[37] In these references, instead of using the Maxwell-Betti reciprocal work theorem, it was proposed to consider the principle of virtual work, which represents the weak form of equilibrium. Indeed, an interesting feature of the principle of virtual work is that it is rigorously satisfied *for any* continuous and piecewise differentiable virtual field, thus for an infinite number of such fields. The idea is therefore to combine a unique actual displacement field measured during a test with different but independent virtual displacement fields arbitrarily selected by the user. In the case of linear elasticity and if the actual displacement field is such that all the unknown parameters are involved in the response of the specimen, it can be shown that choosing at least as many independent virtual fields as unknowns leads to a system of linear equations, which directly provides the unknowns after inversion. Compared to the approach based on the Maxwell-Betti reciprocal work theorem, a single test is potentially sufficient with the VFM. In addition, only one actual measurement field affected by noise instead of two is involved, which makes this identification technique more robust. Last but not the least, the principle of virtual work is valid whatever the type of constitutive equations, so even in the case of non-linearities such as large deformations or plasticity, which is not the case of the Maxwell-Betti reciprocal work theorem. These features have led VFM-related research to expand, with mainly three types of contributions. The first type deals with the improvement of the method itself, mainly concerning the choice of the virtual fields[38-44] since this choice directly influences the robustness of the method. The second type concerns applications involving more sophisticated constitutive equations. Anisotropic elasticity for composite materials[45-47] and wood,[48] elasticity or hyperlasticity of elastomers[49,50] and biological materials,[51-54] elastoplasticity of plain metals[55-61] or welds,[62] are typical examples. The use of the VFM to characterize some materials which are less widely used in mechanical engineering, such as paperboard[63] or polymeric foams,[64] has also been reported in recent papers. The effect of time was also considered with vibrations.[65,66] This made it possible to characterize viscoelastic materials.[67,68] Characterizing the response of various materials at high strain rates constitutes the most recent example of use of this identification method.[69,70] Full details on the VFM can be found in Pierron and Grédiac.[71]The third type of papers on the VFM deals with test design, which is the topic addressed herein.

2.3 | VFM versus FEMU

Some comparisons between FEMU and VFM have been published in different papers.[51,72-76] FEMU may potentially work with a limited number of input data, while full-field measurements are necessary with VFM. Volume integrals involving data in the bulk must be calculated with the VFM, but only measurements at the surface are generally available, except in the cases where digital volume correlation or other bulk measurement techniques like magnetic resonance elastography are available.[77,78] This means that assumptions are required to deduce the through-thickness strain distribution from the measurements on the surface. Such assumptions are reasonable only in the case of thin specimens, while more complex 3D specimens can only be treated with FEMU. Another point is that representative boundary conditions have to be used with finite element calculations, but they are not always available. On the other hand, no exact knowledge of boundary conditions is needed with the VFM if suitable virtual fields are selected. The quality of the results (in terms of robustness) obtained with both identification techniques is globally similar, but the main advantage of the VFM is that no resolution of the direct problem is necessary, which considerably reduces computation times. As an example, it was reported that for comparable identification performance, the VFM was 125 times faster than FEMU in the case of biomaterials exhibiting a hyperelastic response[51] and 428 or 263 times faster for two cases of elastoplasticity.[79] With a view to designing optimal testing conditions, it is clear that refining specimen shape or loading configuration requires many resolutions of the parameter identification problem. In that case, reduced computation times for the identification procedure becomes a significant asset.

Let us now examine in which way FEMU and the VFM have been used for designing tests in the literature.

3 | DESIGN BY INTUITION

A simple route to obtain heterogeneous strain fields is to 'recycle' pre-existing tests, by keeping them as such or by slightly adapting them. For instance, in one of the very first papers on this topic,[20] it was proposed to perform a tensile test on a parallelepipedic specimen. Heterogeneity was induced by two asymmetric notches machined on each side of

the specimen. The in-plane displacement was measured with a video tracking system, at 120 retro-reflective markers regularly deposited onto the front face of the specimen. From these measured displacements, the authors identified the yield stress of both the isotropic Von Mises and the orthotropic Hill yield criteria by using FEMU. A similar specimen geometry was discussed in Pottier et al.[22] with the same objective, but DIC was used in this case to perform the measurements. In Guner et al.,[80] heterogeneity was induced by a varying cross-section and the planar anisotropy of the plastic response was identified. Another intuitive approach is to use an open-hole tensile test[81-84] as the specimens are easy to manufacture and provide strain heterogeneity. The displacement field, measured with ESPI (electronic speckle pattern interferometry) in Lecompte et al.,[81] DIC in Silva et al. and Kowalczyk[82,83] and moiré interferometry in Gogu et al.,[84] was used to feed FEMU with experimental data and identify the four in-plane stiffnesses of an orthotropic composite material. The authors of the latter reference note that various sources of uncertainty impair the quality of the results and thus pay attention to quantifying the uncertainty with which the parameters are identified by using a Bayesian approach. A double notched specimen was also employed in Kowalczyk,[83] and the authors observed that Poisson's ratio was more easily identified with this second geometry.

An extension of the classical tensile test is the biaxial tensile test, which gives rise to a heterogeneous strain field at the centre of cruciform specimens. This test has been used in various cases in the literature:

- Composite materials have been characterized in Lecompte et al.[85] by using DIC and FEMU. Results from specimens with and without a hole in the centre are compared. Interestingly, the authors report that results are better without the hole, presumably because of the bias due an insufficient spatial resolution arising from the concentrated strains around the hole. This remark justifies that a complete optimization procedure for test design should ideally account for the metrological performance of the measuring technique, as discussed in Section 6 below.
- The parameters of a hyperelastic law of an elastomeric material are identified in Promma et al.[49] with DIC and VFM. Compared to the preceding case, the strain level is much higher, which makes the signal-to-noise ratio more favourable.
- The parameters governing an elastoplastic law were identified in Cooreman et al.[86] and Bertin et al.[87] The geometry of the fillets between the branches of a cruciform specimens was adjusted in the latter reference to improve the quality of the identification procedure, and IDIC[24] was employed.

Characterizing plasticity parameters of a mild steel was proposed in Mahnken and Stein[88] by using a compact tension specimen (CT). This test is generally employed to study crack propagation in metals. In this reference, the authors took advantage of the strongly heterogeneous strain field which occurs in such specimens, in order to identify the parameters of a viscoplastic power law with isotropic hardening. The identification method is FEMU and displacement/strain fields were measured by tracking the intersection points between the lines of a grating deposited onto the specimen before the test. More recently, a 'bridge-like' specimen was used in conjunction with the VFM[89] to identify a Hill48 anisotropic plasticity criterion. Unfortunately, the steps to reach this configuration are not detailed in the paper.

The three-point bending test has also been widely used to characterize materials in experimental mechanics. Short beam bending activates the whole set of parameters governing the in-plane response of orthotropic composites, leading to possible identification as illustrated in previous works[27,28,30,90,91] with DIC and FEMU.

Another similar approach is to rely on a standardized shear test developed for composites, namely, the Iosipescu, or double V-notch, shear test. The standard specimen geometry features a double symmetric notch in the gauge section to ensure a dominant and near-uniform strain field between the two notches.[92]In the same vein as for the tensile and bending tests discussed above, this shear test has been recycled by using the standard fixture but removing the specimen notches in an attempt to create a combined state of bending and shear. This specimen thus behaves like a short double-clamped beam. As such and despite the dominance of the shear strain, the four stiffnesses of an orthotropic composite influence the strain field between the clamps. This property has been taken advantage of to characterize various orthotropic materials such as composites[93,94] or wood,[95] the VFM being the identification technique in these cases. It is worth noting that in the latter case, an off-axis configuration was used to enhance identifiability, as also favoured in Kretschmann et al.[96]

Compression of a circular disk (referred to as the Brazilian test) is a well-known test for brittle materials such as rock or concrete. Cao and Xie[97] showed that the heterogeneous strain field observed with moiré interferometry during this test could be used to characterize an orthotropic carbon fibre composite. In Huchzermeyer and Becker,[98] it was proposed to use slotted disks to increase heterogeneity in the strain field and to deduce Young's modulus and Poisson's ratio of an isotropic material.

In conclusion, while sidetracking standard tests to adapt them to the new paradigm of MT2.0 is a first natural approach, it generally falls short when more complex behaviours have to be identified as it is less intuitive to ensure that all parameters are involved in the response. Also, even when identification is successful, the configurations are generally sub-optimal and a more rational approach to test design has to be devised.

4 | DESIGN BY STRAIN STATE

The aim here is to present some examples of test design found in the literature, which are governed by the fact that certain types of strain states should take place within a specimen to activate all the unknown parameters for successful identification. The design variables are mainly some parameters which govern the shape of the specimen after suitable parametrization, the fixture being then adjusted to enable attachment of and load transfer to the specimen. Compared to the preceding examples, non-conventional specimens and/or loading systems are used, and finite element computations are employed to optimize design variables and check that the desired strain states are obtained. This category has been divided into two subcategories: test configurations designed intuitively on strain distribution, and test configurations obtained through actual shape optimization with strain-distribution-based cost function.

4.1 | Intuition-led design based on strain state

A few examples of test designs based on strain states can be found in the literature, where unusual specimen shapes have been intuitively defined based on considerations on strain states. One of the examples deals with a punch test designed to identify an anisotropic Hill48 surface coupled to a Ludwig strain hardening model.[99] The specimen was designed in such a way that various relevant strain states coexisted, each of them occurring in a different part of the specimen. These strain states are biaxial tension, uniaxial tension and shear. Figure 1shows the geometry of the

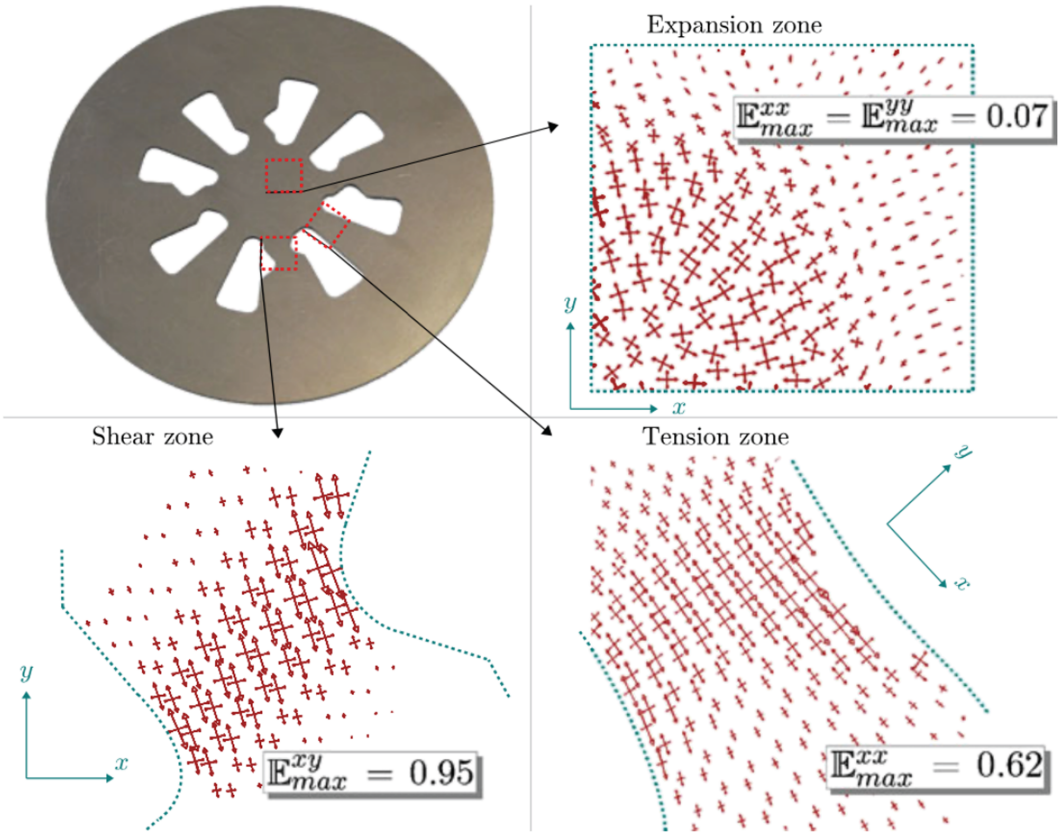

FIGURE 1 Specimen designed for punch test, after Pottier et al.[99] E^{xx}, E^{yy} and E^{xy} are the in-plane components of the Green-Lagrange strain tensor

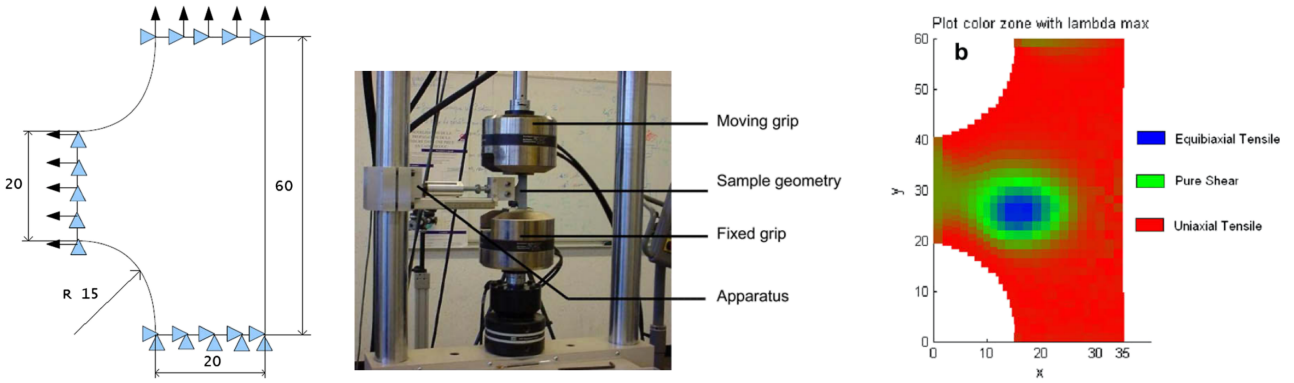

(a) Model of the specimen (b) Testing device (c) Three strain states in the specimen

FIGURE 2 Test design for elastomeric materials where uniaxial tensile (UT), pure shear (PS) and equibiaxial tensile (ET) strain coexist, after Guélon et al.[101]

specimen as well as the strain field obtained with a finite element model. The outer periphery of the specimen is clamped while the load is applied at the centre, perpendicular to the plate, as in a punch test. The specimen is circular, so measurements along both the rolling and transverse directions are possible with the same specimen. DIC was used to measure the 3D displacement and strain at the surface of the specimen, and six constitutive parameters were identified with displacement- and force-based FEMU, two for the Ludwig hardening (the initial yield stress was obtained separately), and four for the Hill48 criterion. This test configuration was used recently by other authors to calibrate a Yld2000 anisotropic criterion.[100]

In the same spirit, hyperelastic materials were considered in Guélon et al.[101] Classically, three homogeneous tests are performed to characterize hyperelastic materials, namely, uniaxial tensile (UT), pure shear (PS) and equibiaxial tensile (ET) tests.[102] Note that the three corresponding strain states coexist in the biaxial test discussed in the preceding section, but in Guélon et al.,[101] it was proposed to combine these three types of strain states in a single test which derives from the classic tensile test, merely by adding to the specimen a third branch perpendicular to the two of the classic geometry of any tensile specimen; see Figure 2a. Compared to the biaxial test on cruciform specimens, the benefit is to obtain these three strain states with a uniaxial tensile machine, which is more readily available in testing labs than a biaxial one. This third branch was attached to a grip fixed to the frame of the test machine; see Figure 2b. Simulations confirmed the coexistence of these three strain states at the centre of the specimen; see Figure 2c. According to Guélon et al.,[101] processing the test images with DIC and identifying the parameters with the VFM provided constitutive parameters in agreement with those obtained with classical homogeneous tests.

An appealing aspect of MT2.0 is that specimens featuring non-standard geometries can be tested, thus enabling the measurement of actual properties of components instead of those measured on specimens elaborated specifically for

FIGURE 3 Compression test on a ring cut in a composite tube, after Moulart et al.[103]

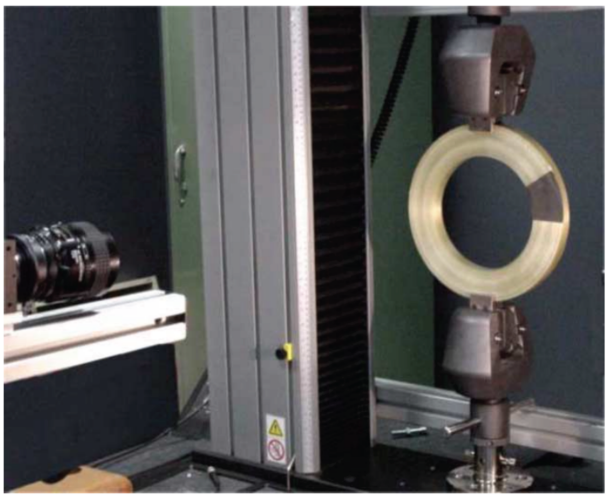

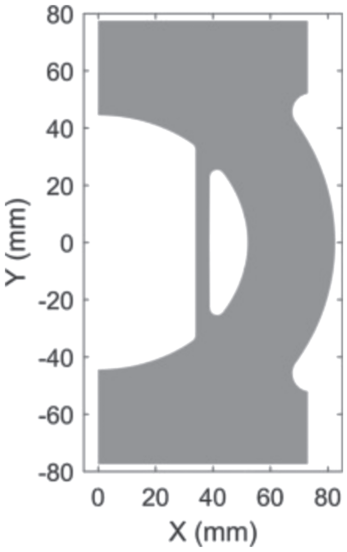

FIGURE 4 Specimen geometry proposed in Jones et al.[105] to identify viscoplastic parameters

testing purposes. This is especially relevant in the case of materials which properties are sensitive to the manufacturing process. In Moulart et al.,[103] for instance, it was proposed to measure the elastic through-thickness parameters of thick composites tubes. It is clear that in this case, even cutting parallelepipedic specimens through the thickness of such tubes and testing them with classical homogeneous tests is irrelevant because of the curvature of the fibres. In Moulart et al.,[103] it was proposed to cut a thin ring in such tubes, to test it under compression, and to consider only a portion of this ring to perform identification; see the grey zone in Figure 3 below. The location of this zone on the ring has been chosen in such a way that the amplitude of the three in-plane strain components are balanced on average. The aim was to ensure better use of the camera pixels as imaging a larger part of the ring, or even its entirety, would result in the loss of many pixels thus challenging spatial resolution. The same procedure was employed later to obtain the equivalent orthotropic elastic properties of superconducting winding rings (or 'pancakes'), constitutive of a large MRI magnet.[104]

Finally, a D-shaped specimen was designed in Jones et al.[105] to identify the parameters governing a viscoplastic law. The specimen is plane and its D-shaped geometry is unconventional, as can be seen in Figure 4. It was loaded vertically in tension using a standard uniaxial testing machine. This geometry was defined manually but iteratively, starting with a shape chosen by intuition, then by performing FE calculations with a set of constitutive parameters equal to the reference ones, and finally by analysing the results in such a way that various criteria were satisfied in the best possible way. These criteria are that stress and strain rate heterogeneities are maximized, gradients in stress or strain near sample edges are minimized, and buckling is prevented. The authors processed FE simulated data. They found a significant difference between the identified and reference parameters, because of uniqueness issues. This problem was fixed by either reducing the number of unknown parameters or, more satisfactorily, by considering a second test in addition to the first one. This second test was performed by applying a displacement to the moving grip with a higher velocity, which increased the richness of the simulated data input into the identification process. No experimental validation has been published so far.

4.2 | Optimization-led design based on strain state

To the best of the authors' knowledge, the first published application of this approach concerns the optimization of the dimensions of a T-shaped specimen for orthotropic composite materials.[106] The idea here was to combine a bending test on short beam and a tensile test. The former activates the Young modulus in the horizontal direction as well as the in-plane shear modulus, the latter the Young modulus along the vertical direction as well as one of the Poisson's ratios, thus making it possible to identify the four parameters of an orthotropic material on a single test specimen. In Grédiac and Pierron,[106] the dimensions of the specimen a, b, c, d (see Figure 5) were adjusted in such a way that the strain levels over the different zones were balanced. This was achieved by minimizing the following cost function with respect to the design variables:

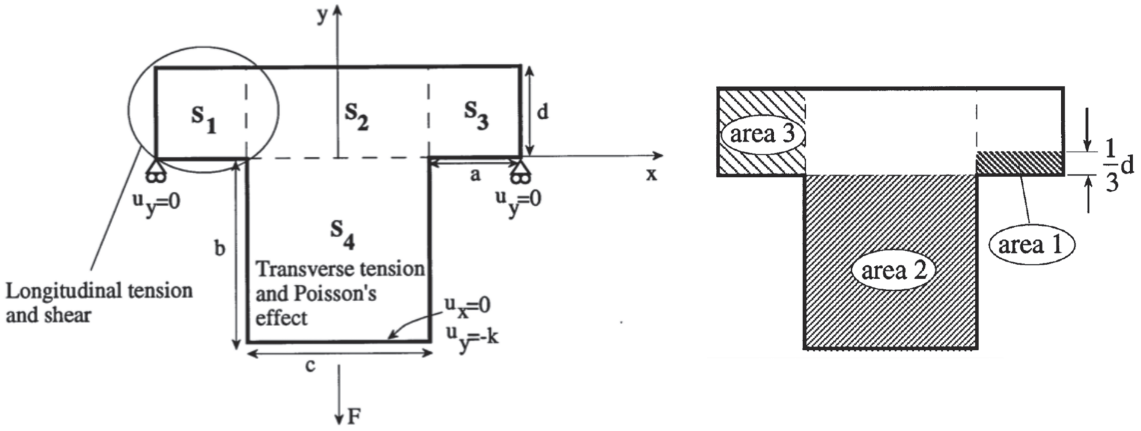

FIGURE 5 Schematic view of the T-shaped specimen (left), and areas for strain balancing (right) after Grédiac and Pierron[106]

$$f\left(\frac{b}{a},\frac{c}{a},\frac{d}{a}\right)=\frac{\left(\overline{\varepsilon_{yy}}-\overline{\varepsilon_{xx}}\right)^2}{\left(\overline{\varepsilon_{yy}}+\overline{\varepsilon_{xx}}\right)}+\frac{\left(\overline{\varepsilon_{yy}}-2\overline{\varepsilon_{xy}}\right)^2}{\left(\overline{\varepsilon_{yy}}+2\overline{\varepsilon_{xy}}\right)}+\frac{\left(\overline{\varepsilon_{yy}}-2\overline{\varepsilon_{xy}}\right)^2}{\left(\overline{\varepsilon_{yy}}+2\overline{\varepsilon_{xy}}\right)}, \tag{1}$$

with a acting as a scaling parameter. $\overline{\varepsilon_{xx}}$ is the average of ε_{xx} over area 1, $\overline{\varepsilon_{yy}}$ the average of ε_{yy} over area 2 and $\overline{\varepsilon_{yy}}$ the average of ε_{yy} over area 3; see Figure 5.

The optimization was performed directly in ANSYS 5.1 using their native APDL language. Unsurprisingly, it was shown that optimal dimensions differed depending on the material orthotropy ratios. A further study proposed an experimental implementation of this test[107] where elastic constants obtained from actual T-shaped tests were in good agreement with reference parameters obtained with standard homogeneous tests. The GM was used for the strain maps, and the identification procedure was the VFM with manually defined virtual fields.

The most advanced implementation of a strain-based test design arises from a series of publications by a Portuguese-French team.[108-111] This concerns the identification of the parameters governing the anisotropic Yld2004-18p[112] plasticity model. The test was designed by maximizing five quantities defined in Souto et al.,[108] which reflect some properties that the specimen should ideally exhibit. The first one is that the strain state range within the specimen should be the widest possible. Each strain state was described by the ratio $\frac{\varepsilon_2}{\varepsilon_1}$ between the minor (ε_2) and major (ε_1) strains of an in-plane stress state. Indeed, this ratio represents different strain states (see Figure 6a), and the widest possible difference between the maximum and minimum values of this ratio represents a wanted feature. This criterion is reflected by C_1 in Equation (2) below.

$$\begin{cases} C_1 &= \left(\frac{\varepsilon_2}{\varepsilon_1}\right)_R = \left(\frac{\varepsilon_2}{\varepsilon_1}\right)_{max} - \left(\frac{\varepsilon_2}{\varepsilon_1}\right)_{min} \\ C_2 &= Std\left(\frac{\varepsilon_2}{\varepsilon_1}\right) = \sqrt{\frac{\sum_i^n\left[\left(\frac{\varepsilon}{\varepsilon_1}\right)_i-\mu\left(\frac{\varepsilon_2}{\varepsilon_1}\right)\right]^2}{n-1}} \\ C_3 &= Std(\bar{\varepsilon}^p) = \sqrt{\frac{\sum_i^n(\bar{\varepsilon}_i^p-\mu(\bar{\varepsilon}^p))^2}{n-1}} \\ C_4 &= \varepsilon_{Max}^p = \frac{\bar{\varepsilon}_{test}^p+\bar{\varepsilon}_{tens}^p+\bar{\varepsilon}_{shear}^p+\bar{\varepsilon}_{biaxial}^p+\bar{\varepsilon}_{comp}^p+\bar{\varepsilon}_{plane}^p}{6} \\ C_5 &= Av(\bar{\varepsilon}^p) = \frac{\sum_i^n\bar{\varepsilon}_i^p v_i}{v_t} \end{cases} . \tag{2}$$

A second feature is that the $\frac{\varepsilon_2}{\varepsilon_1}$ ratio should be spread out over a large range of values between the extrema for this ratio shown in Figure 6a and not be concentrated around the mean value. This property is reflected by the standard deviation of the ratio $\frac{\varepsilon_2}{\varepsilon_1}$ throughout the specimen, which gives C_2 in Equation (2), where n is the number of pixels.

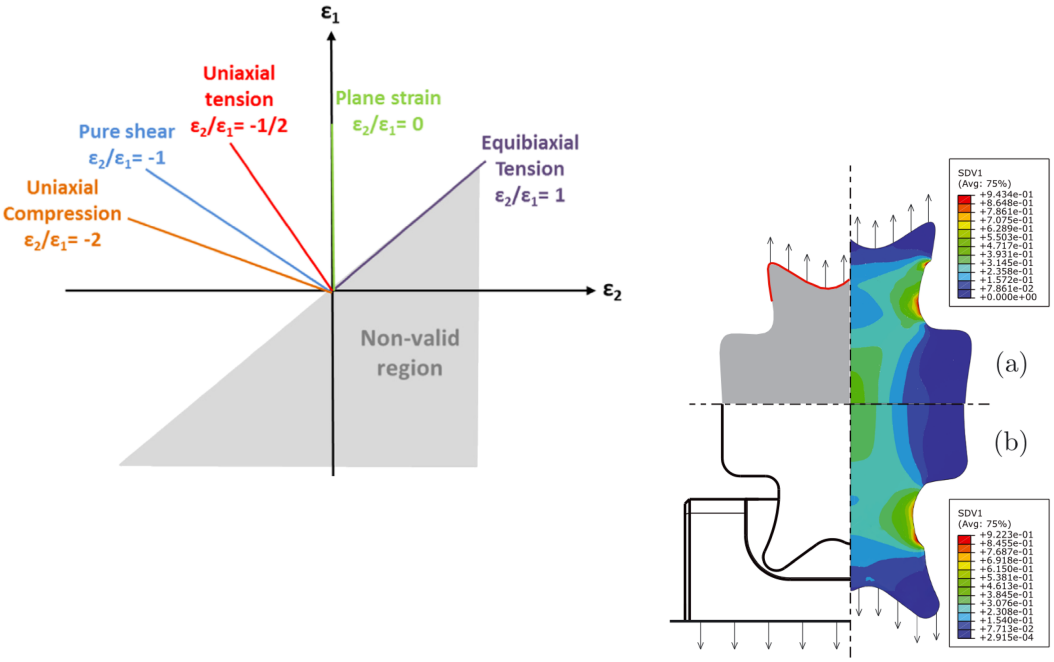

(a) Desired strain states to occur in the specimen, after [108] (b) Butterfly specimen, after [110]

FIGURE 6 Designing a specimen for elastoplasticity, after Souto et al.[108] and Aquino et al.[110]

The heterogeneity of the plastic strain distribution should also be as wide as possible, which means that the standard deviation of the equivalent plastic strain $\bar{\varepsilon}^p$ defined by C_3 in Equation (2) should be maximized.

Since the specimen was designed for sheet metal forming processing, a similar deformation level as the one recorded in actual sheet metal forming should be reached during the test. Hence, the authors proposed to consider a global maximum plastic strain defined by the mean value of the maximum plastic strain achieved during the test on the one hand and the maximum values of the most relevant strain states expected to occur during the test on the other hand, namely, equibiaxial tension, pure shear, uniaxial tension, plane strain tension and uniaxial compression. This gives quantity C_4 in Equation (2).

Finally, the average plastic strain reached within the specimen was also considered because it reflects the global plastic strain level. The points characterized by the highest value are expected to contain the richest information. This quantity is defined by C_5 in Equation (2).

The global criterion was a scaled and weighted sum of the five quantities $C_i, i = 1...5$; thus,

$$I_t = \sum_{1}^{5} \frac{w_{ri} C_i}{w_{ai}}, \tag{3}$$

where where w_{ri} and w_{ai} are relative and absolute weighting factors respectively.

This indicator was then used to rank several test configurations from the literature. In Souto et al.,[109] the process was taken one step further by designing a specimen through the minimization of a cost function built up with this indicator. The specimen edges were defined by control points of a spline function parameterizing the shape, and minimization was performed with respect to the coordinates of these points, using a Nelder-Mead direct search algorithm. In the same spirit, the authors proposed to complete this approach by also designing the shape of the grips through which the load was to be applied to the specimen.[110] This procedure led to the so-called butterfly specimen (see Figure 6b), which has been validated experimentally in Aquino et al.[110] with DIC and FEMU (force and strain cost function) on the Yld2004-18p plasticity model with a Voce hardening function, leading to 18 parameters to identify. In Martins et al.,[111] the VFM was used with the same specimen to identify the Hill48 model with a Swift hardening law.

The same group[113,114] recently extended this approach with a topology optimization tool known as solid isotropic material penalization (SIMP). As opposed to the approach in Souto et al.[109] where the external geometry was

controlled by splines, this starts with a symmetrical rectangular shape and uses a density parameter to give more or less weight to different parts of the sample, with the aim of achieving a binary distribution of density, either 0 or 1, defining the shape of the specimen. This requires a scheme to avoid unrealistic solutions in the form of high frequency variations of the density. Some interesting solutions were found.

5 | DESIGN BY IDENTIFICATION QUALITY

The procedures described above only focus on strain distributions. While they clearly influence the quality of identification, it is difficult to establish a quantitative link between strain distributions and identified quantities without performing the identification. This is why researchers have been trying to use metrics on the quality of identification as a target for test design. In this case, the cost functions driving the test optimization involve identification errors or uncertainties for VFM-based identifications, or FE parameter sensitivities for FEMU identification. The price to pay is that the identification procedure is called in each loop of the iterative design procedure. This type of optimization is therefore much more computationally intensive compared to the use of just strains. Therefore, the computation time of the identification technique becomes a key parameter in this case.

5.1 | Sensitivities to constitutive parameters in FEMU

A natural way to ensure that constitutive parameters are well activated in a particular test is to compute maps of sensitivities of displacement or strain fields to each constitutive parameter. This is done in practice by varying each parameter individually and deriving the sensitivity field by finite difference. This requires at least a number of FE computations equal to twice the number of parameters for a single sensitivity evaluation. It should be noted that in IDIC, the sensitivities are an integral part of the identification process.

To the best knowledge of the authors, the first attempt at test optimization using such sensitivities can be found in Magorou et al.[115] The authors considered bending tests on square wood panels. The location of the supports and applied loads was optimized by maximizing the sensitivity of the deflection of the specimen at the nodes of a regular mesh with respect to each unknown bending rigidity, deflection being estimated with finite element computations. The sensitivity $S(D_{ij})$ of each bending stiffness component D_{ij} is defined by

$$S(D_{ij}) = ||\frac{dU}{dD_{ij}}||/||\frac{U}{D_{ij}}||,\ ij = xx,yy,xy,ss, \tag{4}$$

where $||X||$ denotes the L_2 norm of vector X. D_{xx}, D_{yy}, D_{xy} and D_{ss} are the four orthotropic bending stiffness components. Maximization was performed by using a genetic algorithm. The location of these points being found, an experiment was performed on an Okoume plywood panel. The authors reported that the stiffnesses identified with this procedure were in good agreement with theoretical expectations. The measuring technique for the deflection field was fringe projection and the identified method FEMU with a cost function based on deflections.

More recently, Bertin et al.[116] used sensitivity maps to optimize the fillet radii of a bi-axial cruciform specimen for elastic and elastoplastic identification. It should be noted that for elasticity, a scaling procedure was introduced, which here was the maximum admissible von Mises stress to ensure that the specimen remained fully elastic. Indeed, different geometries exhibit different global stiffnesses, and the sensitivities may be influenced by that. This need for scaling is a recurring issue to optimize tests for elasticity and will be encountered in several studies reported later in this article.

The work presented in Chamoin et al.[117] considers a more advanced shape optimization methodology, SIMP, but still based on FE sensitivities. It was proposed to use IDIC[24] to identify the shear modulus of linear elastic orthotropic materials. The initial specimen shape was rectangular and the load was a uniaxial compression. The specimen was divided into small elements, each of them being affected by a density ρ ranging between 1 and a scalar α, which is positive and close to 0 (and not rigorously 0 to keep the problem well-posed); 0 reflects the total absence of material and 1 its presence. The authors defined the geometry of the specimen by considering the sensitivity of the displacement field to the spatial distribution of ρ. The cost function to be minimized involved both the sensitivity to the shear modulus and the sensitivity to the spatial distribution of ρ. At convergence, a value of ρ close to zero means that the corresponding element should be removed, a value close to one that it should be kept. Numerical simulations carried

with three completely different initial spatial distributions of ρ showed that similar final patterns were obtained at convergence in the three cases. A relatively marked contrast in the distribution of ρ then facilitated the definition of a threshold value beyond which the small ρ-value elements were removed. Only the shear modulus was considered as unknown, the three other constitutive parameters being given a priori. Experiments carried out on an optimized orthotropic wood specimen showed that the shear modulus could be identified with this approach, the sharpness of the cost function around the identified value illustrating the robustness of the procedure.

5.2 | Noise sensitivities in the VFM

In the VFM, FE sensitivities are less relevant as the procedure does not involve any FE computation. In elasticity, the relevant quality indicators are the noise sensitivity parameters η_{ij}, which relate the standard deviation of the strain noise to the standard deviation of each Q_{ij} stiffness parameter as in Avril et al.[118]

$$Std(Q_{ij}) = \eta_{ij}\gamma,\ ij = xx,yy,xy,ss, \tag{5}$$

where γ is the standard deviation of the strain noise, assumed here to be Gaussian, white and uncorrelated between the three strain components. The latter assumption is clearly not rigorous, but it is necessary to solve the problem of virtual field optimization; even if the virtual fields are not optimal stricto sensu, they are still much better than any manually defined ones.

The first study using these noise sensitivity parameters is reported in Pierron et al.[119] where it was proposed to optimize the unnotched Iosipescu specimen discussed in Section 3 with respect to two design variables, the length of the gauge section L and the orientation of the fibres in the specimen, θ, see Figure 7a. The cost function to be minimized is such that the sensitivities η_{ij} are balanced. This cost function is defined by

$$f(L,\theta) = \frac{(\eta_{xx}-\eta_{yy})^2 + (\eta_{xx}-\eta_{ss})^2 - (\eta_{yy}-\eta_{ss})^2}{(\eta_{xx}+\eta_{yy}+\eta_{ss})^2}. \tag{6}$$

η_{xy} was not considered here because its value is always much larger than the others and would therefore have overwhelmed the cost function. The idea of using a normalized cost function is to avoid the problem of scaling. Indeed, since the problem is fundamentally a signal-to-noise ratio one, the procedure would naturally converge towards the stiffest configuration when displacements are imposed, thus leading to the largest possible strain values, regardless of whether they are feasible or not (onset of non-linearity, fracture, poor aspect ratio). In Rossi et al.,[120] this problem was solved by using a maximum stress failure criterion, playing the same role as the von Mises stress in Bertin et al.[116] But here, a scaled cost function was used to mitigate this issue for the sake of simplicity.

Results show that the sensitivity is much higher for θ than for L, as illustrated in Figure 5b where the cost function is nearly flat along the horizontal direction. L was therefore fixed at a reasonable value and θ selected according to the

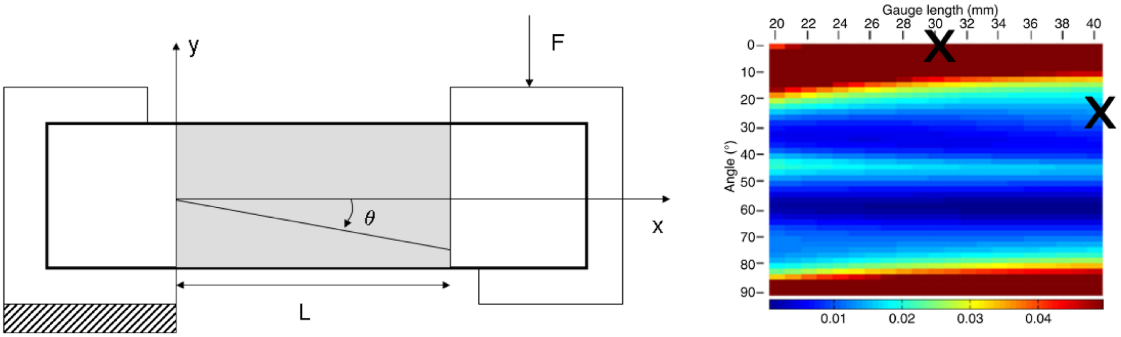

(a) Schematic view of specimen and fixture, after [119]

(b) Cost function and two design points, after [119]

FIGURE 7 Design of an unnotched Iosipescu specimen, after Pierron et al.[119]

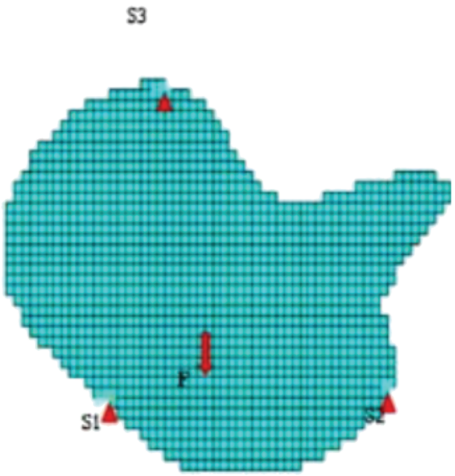

FIGURE 8 Optimization of a bending test for composite plates, after Syed-Muhammad et al.[123]

cost function. Experimental results are presented in Pierron et al.[119] The GM was used as strain measurement technique.

One of the main limitations of this approach is that it does not take into account the resolution of the camera. In fact, preliminary optimizations tended to converge towards very elongated specimens, a trend that can be seen in Figure 7b. This forced the authors to put an upper limit on the specimen length in the optimization process. This is one of the motivations to move to image deformation as presented in the last section.

Other cases of optimal test design based on this approach have been proposed in the literature. For instance, Wang et al.[121] addressed the design of a test for orthotropic foam specimens. The specimen was placed in an Arcan fixture, and both the angle of the fixture with respect to the vertical load and the orientation of the specimen in this fixture were optimized. Data are often missing near the free edges of a test specimen, so the sensitivity of the identified parameters to these missing data was also considered in the optimization procedure. The cost function was similar to that in Equation (6),[119] which meant that no force scaling was necessary as it was embedded in the cost function. It was found that the four stiffnesses (and not only the shear modulus) could be successfully identified with this test when optimized parameters were considered.

In the same spirit, the VFM sensitivity to noise was employed in Muhammad et al.[122] to design a bending test where the six bending stiffnesses of a composite plate were the unknowns. The shape of the plate was parameterized with a spline function. The design variables were the coordinates of the control points of this function, the coordinates of the three supports of the plate and those of the point where the force was to be applied. This led to some non-intuitive shape for the specimen, as well as non-intuitive locations of the supports and applied force, as illustrated in Figure 8. No experimental validation was carried out. This example also shows the limitations of this approach which does not take into account the measurement process. The shape in Figure 8 will lead to the loss of many pixels of the camera, thus challenging the spatial resolution of the measurements.

Finally, in Zhang et al.,[124] it was proposed to optimize an open-hole off-axis specimen subjected to a tensile test in order to identify the four elastic parameters of a unidirectional orthotropic carbon-epoxy composite. The statistical correlation existing between these parameters was also studied. The cost function to be minimized was the sum of the relative difference between reference and identified parameters, and the design variables were the fibre angle and the diameter of the hole. DIC was used to measure the strain field, and the VFM with special optimized virtual fields.[118] The optimal configuration they identified was with the fibres aligned with the specimen length and a hole of 7 mm for a width of 36 mm and a length of 200 mm.

6 | DESIGN BY FULL IDENTIFICATION SIMULATION

In the examples of the preceding section, the data used in the optimization procedure were directly provided by finite element models. However, these data are not exactly equal to the displacement or strain measurements that would be returned by a white-light full-field measurement system such as DIC. Indeed the metrological performance of full-field measurement techniques is now better known, and various types of random and systematic errors impairing the

measurements have been characterized in many recent papers. In particular, a single pixel cannot provide displacement information; it is necessary to rely on the information at the pixels located in a zone surrounding this point. In classical DIC, this zone is a subset, whose shape is generally quadrilateral.[1] When processing regular patterns, various strategies can be employed,[125] but the most popular one is based on the windowed Fourier transform restricted to a single frequency equal to the nominal frequency of the regular pattern, and the window may have various shapes.[126] With both techniques, the consequence is that the displacement returned at a given point also depends on the displacement returned at points located in its vicinity, and the wider the subset or the window, the more marked this dependence. This introduces a bias in the displacement and strain maps, which manifests itself by a blur, thus by the fact that the amplitude of the details and strain gradients are attenuated, as explained, for instance, in Schreier and Sutton[127] and Sur et al.[128] for DIC and Sur and Grédiac[129] for the GM. It also means that considering directly the results of finite element simulations as synthetic experimental data may potentially lead to misleading conclusions when designing optimal testing configurations. For instance, considering these simulations alone may lead to an optimal solution featuring high strain gradients containing rich information, but such gradients may not be correctly rendered by an actual full-field measurement system. Reducing as much as possible the size of the subset for DIC or the window for the GM limits this bias, but the random error due to the fact that images are unavoidably noisy increases in proportion. A trade-off has therefore to be found, and various parameters can be adjusted for that in addition to the size discussed above, such as the degree of the matching function used to model the actual displacement field within the subsets and the step (defined by the distance between two remote subsets) for DIC. The best trade-off should ideally be obtained by adding these settings to the design variables.

Before optimizing all these variables at the same time, intermediate steps have been proposed in the literature. The first one was to simulate the whole chain going from the images to the identified parameters in order to study the influence of various design variables. The first attempt was published in 2012,[130] where synthetic grid images were considered. Displacement and strain fields were extracted from these images and then considered as input data for the VFM. This study was the direct follow-up of that presented in the previous section,[119] where image deformation was not taken into account. The results here showed that a natural minimum appeared in the cost function without having to restrict the range of specimen length. As the procedure naturally takes into account the resolution of the camera, high aspect ratio specimens were penalized and a length of 30 mm was identified as optimal for the unnotched Iosipescu specimen. Since measured displacements are noisy, it is generally necessary to apply some spatial or temporal smoothing before proceeding to differentiation to obtain strains. Such smoothing acts as an additional low pass filter in space, and it is necessary to consider how this operation can be performed in an optimal manner to minimize the bias arising from it. Such optimal displacement smoothing parameters can be selected thanks to the simulator introduced in Rossi and Pierron,[130] and uncertainty bounds for the identified stiffness components can be derived from the process. This simulator was then extended to DIC,[120] unsurprisingly showing the superiority of the performances of the GM, consistent with recent results obtained with a rigorous approach.[131] This simulator with the GM has also been used in transient dynamics to optimize post-processing parameters for the so-called image-based inertial impact (IBII) test.[132] It was used in Bouda et al.[133] to compare three IBII test configurations (a plain one and two others with a hole or notches) for viscoplastic identification of a titanium alloy. The effect of impact speed was also explored, together with spatial and smoothing parameters.

All the links of the chain spanning between synthetic images and final constitutive parameters being available through suitable models, the next stage is to optimize the settings and design variables governing each of these links. This is however quite a complex problem because of (i) the number of parameters to be considered, which is greater than in Section 5 above, and (ii) the fact that some variables such as the subset size for DIC and the degree of the matching function are discrete, which makes it necessary to use more involved optimization procedures like genetic algorithms. This obviously induces significant computation times, the identification procedure being run within each iteration of the optimization procedure.

A first attempt was proposed in Rossi et al.[134] for elastoplastic identification, where the geometry of a double notch machined in a tensile specimen was optimized. Two subset sizes and 25 different combinations of variables defining the notches were considered. The cost function used here was the squared difference between the reference and identified stress-strain curves. The reason for this choice is that the stress-strain curve can be more or less sensitive to some parameters, so only the most influencing ones were considered if choosing this cost function. The best design was the one minimizing the distance between these two stress-strain curves. Interestingly, the best option was shown to be the one leading to a diffuse plastic strain distribution while non-optimal ones exhibited high strain concentration close to the notches, which was probably due to the fact that high strain gradients were poorly rendered by the DIC system. As

in Bouda et al.,[133] this approach was however only a comparison between potential candidates defined a priori, so the procedure probably missed some better configurations.

A more sophisticated approach was presented in Gu and Pierron[135] to tackle this problem by using a two-step approach. Indeed the geometry and the load were first optimized by using fixed (but reasonable) values for the DIC settings. The first set of design variables defining the geometry and load were then fixed after this first step, and DIC parameters were optimized in a second step. Different tests were considered to identify the parameters governing the elastic behaviour of orthotropic materials like composites, namely, an off-axis tensile test on short specimen (SOAT), a Brazilian test performed on off-axis disks (OABD) and a Iosipescu test on an unnotched off-axis specimen (OAUIT). A hole was also added at the centre of the first type of specimen to examine the benefit of an increased heterogeneity due to this strain concentrator (SOAHT). These different configurations are shown in Figure 9a. Compared to the open-hole tensile specimen proposed in previous studies[81-84] and discussed in Section 3 above, the aspect ratio of the specimen considered here is lower in order to increase heterogeneity, even in the absence of hole. The orientation of the specimen and off-axis angle were first optimized in addition to the diameter of the hole. The C_3 cost function below was used for this optimization, combining systematic (C_1) and random (C_2) errors in C_3 (maximal error within a 95% confidence interval):

$$\begin{cases} C_1 &= \dfrac{1}{4}\displaystyle\sum_{ij}\frac{|Q_{ij}^{id}-Q_{ij}^{ref}|}{Q_{ij}^{ref}} \\ C_2 &= \dfrac{1}{4}\displaystyle\sum_{ij}\frac{\sigma_{ij}^{id^{ref}}}{Q_{ij}} \quad ,ij=11,22,12,66, \\ C_3 &= C_1+2C_2 \end{cases} \tag{7}$$

where *id* denotes an identified stiffness and *ref* the reference one. σ_{ij}^{id} is the standard deviation of Q_{ij}^{id} estimated from images with 30 different copies of a white Gaussian grey level noise. The same maximum stress criterion scaling strategy as in Rossi et al.[120] was used. Figure 9b–e show C_3 as a function of the design variables chosen for each configuration. The main conclusion is that a unique minimum exists in each case, and the variables corresponding to this minimum are those retained to define the optimal test design.

OAUIT was found to be the best candidate after the first optimization step, closely followed by SOAHT. A second step was then designed to optimize DIC processing parameters (subset size and strain window, with step size fixed at 50% of the subset size) to try and reduce the values of the C_3 cost function. Interestingly, the results from the second step change this ranking with SOAHT stepping ahead of OAUIT. This result shows that constraints coming from the measuring system should be taken into account during the design process of optimal tests. Another interesting conclusion of this second step is that quadratic matching functions (instead of bilinear ones) and steps of one pixel between successive subsets should systematically be used, leading to lower values of C_3. The superiority of the quadratic shape functions has been documented in previous works,[136,137] while step size has, regrettably, not been the focus of much attention in the past. It is worth noting that the orientation of the fibres in OAUIT has also been optimized with this type of approach in the particular case of wood, see Kretschmann et al.[96]

In the same spirit as in the preceding study, a refinement of the work presented in Wang et al.[121] on orthotropic polymeric foams (and discussed in the preceding section) tested with an Arcan fixture was proposed in Wang et al.[64] The experimental device is shown in Figure 10. The specimen was bonded onto the surfaces of the Arcan rig which was in turn mounted onto a uniaxial test machine. Optimization was conducted again in two steps. DIC was the measurement method, so reasonable settings were fixed for a first optimization of both the angle of the fixture with respect to the vertical load (α) and the orientation of the specimen in the fixture (θ). Synthetic reference and deformed speckle images were used to obtain displacement and strain maps. These maps were then fed into the optimization procedure. Force scaling was performed using a maximum strain criterion. The second step consisted in considering the optimized configuration defined during the first step, and then in optimizing the DIC settings. This led to an optimal configuration which was different from the one given in Wang et al.[121] The stiffnesses obtained with this approach were similar, but the uncertainty with which they were provided could be predicted only with this more refined approach. Experimental results showed that the standard deviation reflecting this uncertainty were predicted within less than a factor two, which can be considered as satisfactory since other sources of errors than the camera sensor exist when actual experiments are performed, such as microvibrations, light fluctuation, geometrical defects and defects in load introduction and alignment.

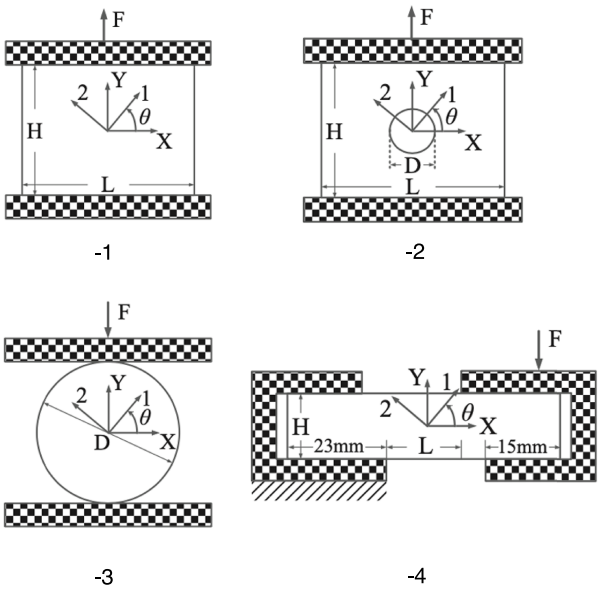

(a) -1 short off-axis tensile test (SOAT), -2 short off-axis open-hole tensile test (SOAHT), -3 off-axis Brazilian disc (OABD) and -4 off-axis unnotched Iosipescu test (OAUIT)

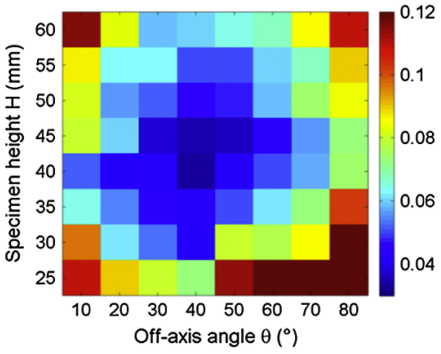

(b) SOAT, influence of H and θ

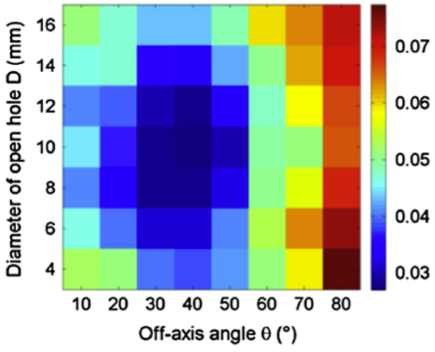

(c) SOAHT, influence of D and θ

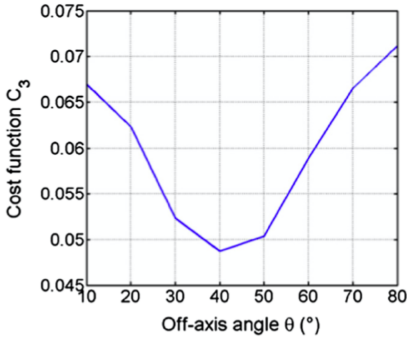

(d) OABD, influence of θ

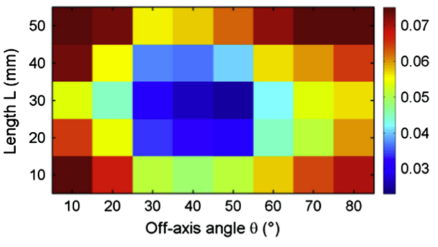

(e) OAUIT, influence of L and θ

FIGURE 9 Four tests for composite characterization and cost function C_3 as a function of various of design variables, after Gu and Pierron[135]

In the examples discussed above, the two-step approach was used only in order to simplify the problem, but it is clear that all the variables should be considered at the same time while optimizing them so that any possible coupling is not missed. A preliminary study has been carried out in Gu and Pierron[138] to reach this goal. The design of the T-shaped specimen addressed in Section 4 was revisited. The total height and width of the specimen were fixed to correspond to the camera sensor aspect ratio, so that the lowest number of pixels are lost. Five design variables were considered to define the geometry of the specimen and the orientation of the material: two geometrical parameters, c and d as defined in Figure 5, the radius of the fillet joining the horizontal and vertical bars of the 'T', the orthotropy

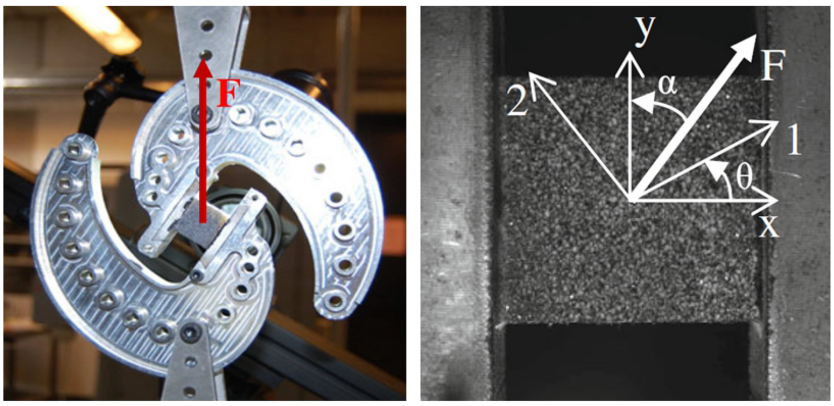

FIGURE 10 Arcan fixture used to test an orthotropic foam specimen, after Wang et al.[121] Both the orientation of the fixture (angle α) and the off-axis angle of the specimen, θ, were optimized, as well as the DIC and smoothing parameters used to extract strain fields from the speckle images by DIC

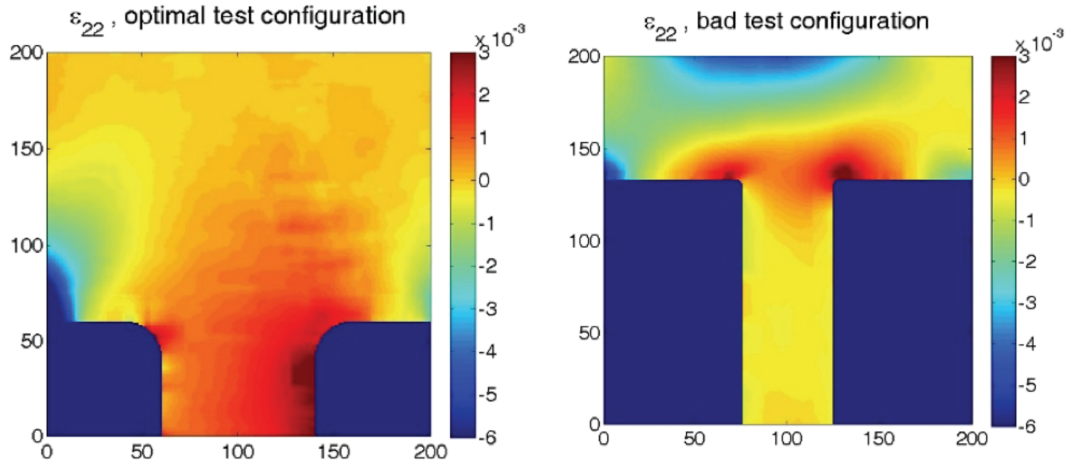

FIGURE 11 T-shaped specimens, after Gu and Pierron,[138] with orthotropy direction at 27° from the horizontal axis for the optimal T, and 70° for the sub-optimal one

angle, the DIC settings, namely, the subset size, the step size, and the degree of the matching functions (linear or quadratic), and the size of the Gaussian filter used to smooth the displacement field prior to differentiation to obtain the strain components. A genetic algorithm was used to minimize cost function C_3 defined above because variables 5 to 7 are discrete while the others are continuous. The maximum stress was again used for scaling purposes.

The optimal shape is shown in Figure 11. It is very interesting to note how the initial idea of the T-shaped specimen (horizontal and shear moduli active in the horizontal bar, and transverse modulus and Poisson's ratio in the vertical bar) has been totally lost in the converged design. Indeed, the identifiability of all orthotropic stiffness components is now ensured by the 'flow' of a tensile stress applied by the short vertical bar into what can be seen as a semi-infinite plane, with the off-axis angle ensuring the richness of the test. Compared to the bad configuration on the right hand-side of the figure, one can first see how the optimization tends to ensure maximal use of the camera pixels to maximize spatial resolution and avoid high strain concentrations at the corners of the T. It is also worth mentioning that the algorithm systematically converged towards a step size of 1 and quadratic shape functions. This was a first approach that would need to be refined by including a buckling criterion to check that the design is not limited by the wide horizontal bar. Experimental validation of this design is still needed.

7 | DISCUSSION AND CONCLUSION

The following remarks can be drawn from the examples shown in the four preceding sections.

- With the maturation of camera-based full-field deformation measurements (DIC, GM), a paradigm shift in the mechanical testing of materials is emerging. Traditional test methods developed for point sensors like strain gauges

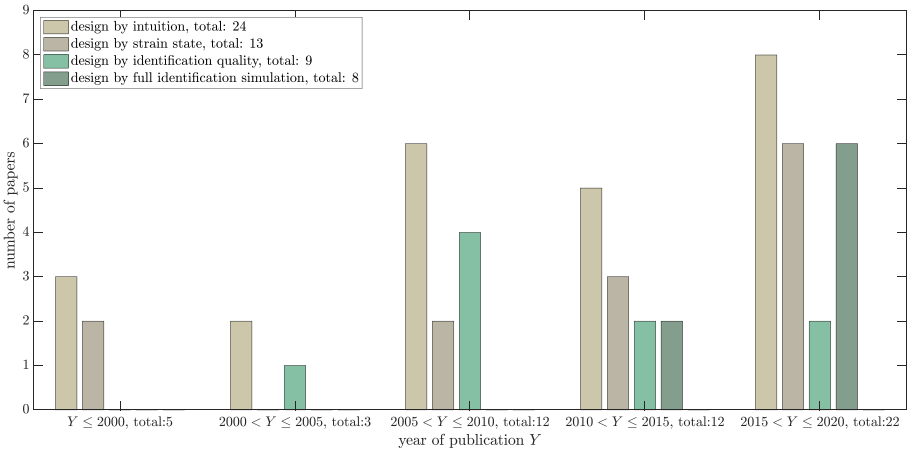

FIGURE 12 Distribution over time of the studies dealing with optimization of tests for Material Testing 2.0, which are cited in the present paper

or extensometers have largely relied on statically determinate configurations, for which a closed-form expression linking the unknown constitutive parameters and local measurements exists. Unfortunately, these tests exhibit strong limitations like the reliance on well-controlled boundary conditions, restricted stress-strain information and difficulties to deal with heterogeneous materials and complex constitutive models that require many tests to be calibrated. In contrast, the wealth of information contained in full-field (or more rigorously, spatially dense) measurements opens up opportunities to design new statically indeterminate tests for more efficient and cost-effective model calibration. It was chosen here to give visibility to this new paradigm by christening it 'Materials Testing 2.0' (MT2.0).

- While early efforts towards MT2.0 focused on the development of full-field measurements and efficient inverse analysis tools (like FEMU and the VFM) to identify constitutive parameters from measured heterogeneous kinematic fields, gradually, researchers are turning towards the design of optimal tests fully adapted to the philosophy of MT2.0. The distribution of the contributions over the years shows that this activity is indeed quite recent, see Figure 12. There is only a limited number of attempts before 2000, but this research field is ramping up. It can be seen that designing by intuition is by far the subject of the largest number of studies. This is logical since this is the first step towards the more sophisticated approaches which have progressively appeared over the years. Interestingly, even recent contributions belong to this first category, certainly because of the arrival of newcomers to this field fuelled by the increased interest from the scientific community in MT2.0.
- Most of the examples deal with anisotropic elasticity, and a few with hyperelasticity and elastoplasticity, which makes room for future improvement in the last two cases. This is especially true for elastoplasticity, where advanced constitutive laws (like the Yld2004-18p anisotropic plasticity model in Barlat et al.[112]) involve an increasingly larger number of parameters.
- Most of the cases discussed above concern the VFM, and this is particularly true when considering the most sophisticated procedures presented in the last cases, where FEMU was used in one case only. This is certainly due to the difference in computational efficiency between FEMU and the VFM. It could be argued that IDIC optimization based on sensitivity maps may be equivalent to the VFM identification simulator as IDIC may automatically incorporate the effects of the systematic errors caused by the lack of camera spatial resolution, though the errors arising from the interplay between the FE and DIC meshes is not entirely clear when these meshes are different.
- The nature of the cost function used to optimize the design parameters (and DIC or GM parameters in Section 6) varies from one example to another. A study solely devoted to the influence of the nature of the cost function on the quality of the results and on the convergence speed should be undertaken, along similar lines to those discussed for the minimization of the optical residual in DIC.[139]
- The last three types of design procedures rely on finite element simulations. Such simulations are performed for a given constitutive law and for a given set of constitutive parameters. It means that the optimal solutions they provide are theoretically optimal for these parameters only, and that changing either the type of constitutive law and/or its constitutive parameters should lead to other solutions, thus limiting the scope of any optimal test obtained for certain parameters and not others. For instance, one particular test can be optimal for glass/epoxy composites used during the simulations, but keeping the same geometry and load with carbon/epoxy composites is probably no longer optimal. This advocates for a systematic exploration of the design space for mechanical tests before new materials are

tested if their properties are too different from previously considered ones. This could be performed through a commercialized software platform dedicated to test design and uncertainty quantification. Some efforts towards this goal are currently underway in a few teams worldwide, but there is no doubt that such tools will be readily available in the near future. This is the adaptation of the notion of digital virtual twin to the MT2.0 paradigm, where each test has its virtual numerical twin used to assess performances and provide uncertainty.

- It is worth noting that only kinematic (displacement, acceleration, slope or strain) measurements are involved in the examples discussed in the four sections above. Thermal fields are also widely used in experimental mechanics, either alone (for instance when performing thermoelastic stress analysis or estimating heat sources at the surface of loaded specimens) or in combination with displacement and strain measurements. Designing tests to exhibit simultaneous kinematic and thermal heterogeneities in order to enrich the experimental database is certainly a promising route.
- Finally, the problem of the assessment of quality of the constitutive model is the large gaping hole in the current state of the art, as also nicely pointed out in Roux and Hild.[76] Novel non-parametric approaches are emerging,[140-143] piecewise-defined models have been explored[60] but in spite of these promising efforts, there is a need for ways of either discriminating between models or formulating models based on MT2.0 methodologies. This is still an open problem.

In conclusion, it can be said that designing mechanical tests for MT2.0 is an emerging research topic, which lies at the frontier between image processing, experimental and computational mechanics. This is confirmed by the increasing number of recent studies on this topic published in the literature, which are briefly reviewed in the present paper. The examples discussed here show that a certain graduation can be identified, with studies ranging between a mere adaptation of pre-existing classical tests to much more sophisticated ones, where even constraints imposed by the measurement technique are accounted for. The price to pay is the increasing computational resources needed when going from the former to the latter. Recent advances on inverse techniques devoted to identification from full-field measurements on the one hand, and on the metrological performance of full-field measurement techniques on the other hand, now forge a solid footing for MT2.0, which means that optimizing mechanical tests dedicated to this type of approach should attract more researchers in the near future and will hopefully penetrate industry, and lead to new standards in the future.

ORCID

F. Pierron https://orcid.org/0000-0003-2813-4994
M. Grédiac https://orcid.org/0000-0002-6814-1438

REFERENCES

[1] M. Sutton, J. J. Orteu, H. Schreier, *Image Correlation for Shape, Motion and Deformation Measurements. Basic Concepts, Theory and Applications*, Springer **2009**.
[2] M. Grédiac, F. Sur, B. Blaysat, *Strain* **2016**, *52*, 205.
[3] S. A. Masroor, L. W. Zachary, *Exp. Mech.* **1991**, *31*, 33.
[4] D. K. Gupta, A. K. Dhingra, *Mech. Syst. Signal Process.* **2005**, *40*, 556.
[5] P. C. Shah, F. E. Udwadia, *J. Appl. Mech.* **1977**, *45*, 188.
[6] P. H. Kirkegaard. **1991**, Ph.D. Thesis.
[7] D. C. Kammer, M. L. Tinker, *Mech. Syst. Signal Process.* **2004**, *18*, 29.
[8] M. Meo, G. Zumpano, *Eng. Struct.* **2005**, *27*, 1488.
[9] V. V. Ferodov, *Theory of Optimal Experiments*, Academic Press, New York and London **1972**.
[10] D. Y. Oh, H. C. No, *Nucl. Eng. Des.* **1994**, *152*, 197.
[11] R. Naimimohasses, D. M. Barnett, D. A. Green, P. R. Smith, *Meas. Sci. Technol.* **1995**, *6*, 1291.
[12] L. Padula, D. Palumbo, R. Kincaid, Optimal sensor/actuator locations for active structural acoustic control, *Technical report*, NASA Langley Technical Report Server **1998**.
[13] M. Vitse, M. Poncelet, A. E. Iskef, J. E. Dufour, R. Gras, A. Bouterf, B. Raka, C. Giry, F. Gatuingt, F. Hild, *J. Strain Anal. Eng. Des.* **2020**. Accepted, in press.
[14] L. X. Huang, Z. H. Xiang, X. S. Sun, Y. H. Liu, Z. Z. Cen, *Comput. Mech.* **2006**, *38*, 201.
[15] K. T. Kavanagh, R. W. Clough, *Int. J. Solids Struct.* **1971**, *7*, 11.
[16] K. T. Kavanagh, *Exper. Mech.* **1972**, *12*, 50.
[17] R. M. Courtade, P. Hamelin, J. C. Cubaud, *Fibre Sci. Technol.* **1975**, *8*, 207.
[18] C. W. J. Oomens, M. R. Ratingenv, J. D. Janssen, J. J. Kok, M. A. N. Hendriks, *J. Biomech.* **1993**, *26*, 617.
[19] G. Boyer, J. Molimard, M. B. Tkaya, H. Zahouani, M. Pericoi, S. Avril, *J. Mech. Behav. Biomed. Mater.* **2013**, *27*, 273.

[20] M. H. H. Meuwissen, C. W. J. Oomens, F. P. T. Baaijens, R. Petterson, J. D. Janssen, *J. Mater. Process. Technol.* **1998**, *75*, 204.
[21] J. Kajberg, G. Lindkvist, *Int. J. Solids Struct.* **2004**, *41*, 3439.
[22] T. Pottier, F. Toussaint, P. Vacher, *Eur. J. Mech. - A/Solids* **2011**, *30*, 373.
[23] J. Réthoré, T. E. Muhibullah, M. Coret, P. Chaudet, A. Combescure, *Int. J. Solids Struct.* **2013**, *50*, 73.
[24] F. Mathieu, H. Leclerc, F. Hild, S. Roux, *Exper. Mech.* **2015**, *55*, 105.
[25] A. P. Ruybalid, J. P. M. Hoefnagels, O. vander Sluis, M. arcG. D. Geers, *Int. J. Numer. Methods Eng.* **2016**, *106*, 298.
[26] F. Amiot, F. Hild, J. P. Roger, *Int. J. Solids Struct.* **2007**, *44*, 2863.
[27] Y. He, A. Makeev, B. Shonkwiler, *Composites Sci. Technol.* **2012**, *73*, 64.
[28] A. Makeev, Y. He, P. Carpentier, B. Shonkwiler, *Composites Part A: Appl. Sci. Manuf.* **2012**, *43*, 2199.
[29] J. C. Passieux, F. Bugarin, C. David, J. N. Périé, L. Robert, *Exper. Mech.* **2015**, *55*, 121.
[30] T. He, L. Liu, A. Makeev, B. Shonkwiler, *Composite Struct.* **2016**, *140*, 84.
[31] M. Kroon, *J. Comput. Appl. Math.* **2010**, *234*, 563.
[32] S. Drapier, I. Gaied, *Inverse Probl. Sci. Eng.* **2007**, *15*, 871.
[33] J. Réthoré, P. Simon, H. Maigre, in Proceedings of the 14th International Conference on Experimental Mechanics (ICEM 14), *6* **2010**:7.
[34] J. F. Witz, S. Roux, F. Hild, J. B. Rieunier, *J. Eng. Mater. Technol.* **2008**, *130*, 7.
[35] A. Foudjet. **1986**, Ph.D. Thesis, INSA Lyon.
[36] M. Grédiac, *Comptes Rendus de l'Académie des Sci.* **1989**, *309-II*, 1. Gauthier-Villars.
[37] M. Grédiac, A. Vautrin, *J. Appl. Mech.* **1990**, *57*, 964.
[38] M. Grédiac, E. Toussaint, F. Pierron, *Int. J. Solids Struct.* **2002**, *39*, 2691.
[39] S. Avril, M. Grédiac, F. Pierron, *Comput. Mech.* **2004**, *34*, 439.
[40] T. T. Nguyen, J. M. Huntley, I. A. Ashcroft, P. D. Ruiz, F. Pierron, *Strain* **2014**, *50*, 454.
[41] A. Marek, F. M. Davis, F. Pierron, *Comput. Mech.* **2017**, *60*, 409.
[42] A. Marek, F. M. Davis, M. Rossi, F. Pierron, *Int. J. Mater. Forming* **2019**, *12*, 457.
[43] A. Tayeb, J.-B. L. Cam, M. Grédiac, E. Toussaint, E. Robin, X. Balandraud, F. Canevet, Sensitivity-based virtual fields for identifying hyperelastic constitutive parameters, Submitted, **2019**.
[44] A. Marek, F. M. Davis, J. H. Kim, F. Pierron, *Exper. Mech.* **2020**, *60*, 639
[45] M. Grédiac, A. Vautrin, G. Verchery, *J. Appl. Mech.* **1993**, *60*, 614.
[46] H. Chalal, S. Avril, F. Pierron, F. Meraghni, *Composites Part A: Appl. Sci. Manuf.* **2006**, *37*, 315.
[47] R. Moulart, S. Avril, F., Pierron, *Composites Part A: Appl. Sci. Manuf.* **2006**, *37*, 326.
[48] J. Xavier, F. Pierron, *J. Strain Anal. Eng. Des.* **2018**, *53*, 556.
[49] N. Promma, B. Raka, M. Grédiac, E. Toussaint, J. B. L. e Cam, X. Balandraud, F. Hild, *Int. J. Solids Struct.* **2009**, *46*, 698.
[50] T. Guélon, E. Toussaint, J.-B. L. e Cam, N. Promma, M. Grédiac, *Polymer Test.* **2009**, *28*, 715.
[51] L. Zhang, S. G. Thakku, M. R. Beotra., M. Baskaran, T. Aung, J. C. H. Goh, N. G. Strouthidis, M. J. A. Girard, *Biomech. Model. Mechanobiol.* **2017**, *16*, 871.
[52] S. Avril, P. Badel, A. Duprey, *J. Biomech.* **2010**, *43*, 2978.
[53] F. Meng, X. Zhang, J. Wang, C. Li, J. Chen, C. Sun, *Appl. Sci.* **2019**, *9*, 1349.
[54] R. Miller, A. Kolipaka, M. P. Nash, A. A. Young, *Int. J. Numer. Methods Biomed. Eng.* **2018**, *34*, 2979.
[55] M. Grédiac, F. Pierron, *Int. J. Plasticity* **2006**, *26*, 602.
[56] J.-H. Kim, A. Serpantié, F. Barlat, F. Pierron, M.-G. Lee, *Int. J. Solids Struct.* **2013**, *50*, 3829.
[57] J. Fu, F. Barlat, J.-H. Kim, F. Pierron, *Int. J. Solids Struct.* **2016**, *102-103*, 30.
[58] M. Rossi, F. Pierron, M. Stamborska, *Int. J. Solids Struct.* **2016**, *97–98*, 322.
[59] J. M. P. Martins, A. G. Andrade-Campos, S. Thuillier, *Int. J. Solids Struct.* **2019**, *172-173*, 21.
[60] M. Rossi, A. Lattanzi, F. Barlat, *Strain* **2018**, *54*, e12265.
[61] G. Valeri, B. Koohbor, A. Kidane, M. A. Sutton, *Opt. Lasers Eng.* **2017**, *91*, 53.
[62] G. L. e Louëdec, F. Pierron, M. A. Sutton, A. P. Reynolds, *Exper. Mech.* **2013**, *53*, 849.
[63] J. M. Considine, F. Pierron, K. T. Turner, D. W. Vahey, *Exper. Mech.* **2014**, *54*, 1395.
[64] P. Wang, F. Pierron, M. Rossi, P. Lava, O. T. Thomsen, *Strain* **2016**, *52*, 59.
[65] M. Grédiac, P.-A. Paris, *J. Sound Vibr.* **1996**, *195*, 401.
[66] M. Grédiac, N. Fournier, P.-A. Paris, Y. Surrel, *J. Sound Vibr.* **1998**, *210*, 645.
[67] A. Giraudeau, F. Pierron, *J. Sound Vibr.* **2005**, *284*, 757.
[68] A. Giraudeau, B. Guo, F. Pierron, *Exper. Mech.* **2006**, *46*, 777.
[69] R. Seghir, F. Pierron, *Exper. Mech.* **2018**, *58*, 183.
[70] F. Pierron, H. Zhu, C. Siviour, *Philos. Trans. R. Soc. A Math.* **2014**, *372*, 20130195.
[71] F. Pierron, M. Grédiac, *The Virtual Fields Method*, Springer **2012**.
[72] S. Avril, F. Pierron, *Int. J. Solids Struct.* **2007**, *44*, 4978.
[73] S. Avril, M. Bonnet, A. S. Bretelle, M. Grédiac, F. Hild, P. Ienny, F. Latourte, D. Lemosse, S. Pagano, S. Pagnacco, F. Pierron, *Exper. Mech.* **2008**, *48*, 381.
[74] E. Markiewicz, B. Langrand, D. Notta-Cuvier, *Int. J. Impact Eng.* **2017**, *110*, 371.

[75] J. M. P. Martins, S. Thuillier, A. G. A Campos, in 21st International ESAFORM Conference on Material Forming (ESAFORM) **2018**. https://hal.archives-ouvertes.fr/hal-02069341
[76] S. Roux, F. Hild, *Int. J. Solids Struct.* **2020**, *184*, 14.
[77] F. Gillard, R. Boardman, M. Mavrogordato, D. Hollis, I. Sinclair, F. Pierron, M. Browne, *J. Mech. Behav. Biomed. Mater.* **2014**, *29*, 480.
[78] N. Connesson, E. H. Clayton, P. V. Bayly, F. Pierron, *Strain* **2015**, *51*, 110.
[79] J. M. P. Martins, A. G. Andrade-Campos, S. Thuillier, *Int. J. Mech. Sci.* **2018**, *145*, 330.
[80] A. Guner, C. Soyarslan, A. Brosius, A. E. Tekkaya, *Int. J. Solids Struct.* **2012**, *49*, 3517.
[81] D. Lecompte, H. Sol, J. Vantomme, A. M. Habraken, in Proceedings of the SEM Annual Conference and Exposition on Experimental and Applied Mechanics **2005**.
[82] G. Silva, R. L. e Riche, J. Molimard, A. Vautrin, C. Galerne, *Appl. Mech. Mater.* **2007**, *7-8*, 73.
[83] P. Kowalczyk, *Measurement* **2019**, *135*, 131.
[84] C. Gogu, W. Yin, R. Haftka, P. Ifju, J. Molimard, R. LeRiche, A. Vautrin, *Exper. Mech.* **2013**, *53*, 635.
[85] D. Lecompte, A. Smits, H. Sol, J. Vantomme, D. V. Hemelrijck, *Int. J. Solids Struct.* **2007**, *44*, 1643.
[86] S. Cooreman, D. Lecompte, H. Sol, J. Vantomme, D. Debruyne, *Exper. Mech.* **2008**, *48*, 421.
[87] M. Bertin, F. Hild, S. Roux, F. Mathieu, H. Leclerc, P. Aimedieu, *J. Strain Anal. Eng. Des.* **2016**, *51*, 118.
[88] R. Mahnken, E. Stein, *Comput. Methods Appl. Mech. Eng.* **1996**, *136*, 225.
[89] J. Fu, W. Xie, L. Qi, *Proc. Manuf.* **2020**, *47*, 812.
[90] R. Gras, H. Leclerc, S. Roux, S. Otin, J. Schneider, *Exper. Mech.* **2013**, *53*, 719.
[91] Z. Liu, L. Liu, T. He, *IOP Conf. Ser.: Mater. Sci. Eng.* **2020**, *751*, 12055.
[92] D. E. Walrath, D. F. Adams, *Exper. Mech.* **1983**, *23*, 105.
[93] F. Pierron, M. Grédiac, *Composites/Part A* **2000**, *31*, 309.
[94] H. Chalal, S. Avril, F. Pierron, F. Meraghni, *Composites Part A: Appl. Sci. Manuf.* **2006**, *37*, 315.
[95] J. Xavier, S. Avril, F. Pierron, J. Morais, *Composites Part A: Appl. Sci. Manuf.* **2009**, *40*, 1953.
[96] D. E. Kretschmann, J. M. Considine, F. Pierron. In: C. Sciammarella, J. Considine, P. Gloeckner, eds. *Experimental and Applied Mechanics*, Conference Proceedings of the Society for Experimental Mechanics Series, vol. 4: Springer, Cham; **2016**:67–76.
[97] Q. K. Cao, H. M. Xie, *Exper. Mech.* **2018**, *58*, 783.
[98] R. L. Huchzermeyer, T. H. Becker, *Exper. Techniques* **2018**, *42*, 671.
[99] T. Pottier, P. Vacher, F. Toussaint, H. Louche, T. Coudert, *Exper. Mech.* **2012**, *52*, 951.
[100] Z. Wang, S. Zang, X. Chu, S. Zhang, L. Leotoing, *Results Phys.* **2019**, *15*, 102655.
[101] T. Guélon, E. Toussaint, J.-B. L. e Cam, N. Promma, M. Grédiac, *Polymer Test.* **2009**, *28*, 715.
[102] G. A. Holzapfel, *Nonlinear Solid Mechanics. A Continuum Approach for Engineering*, J. Wiley and Sons, Chichester **2000**.
[103] R. Moulart, S. Avril, F. Pierron, *Composites Part A: Appl. Sci. Manuf.* **2006**, *37*, 326.
[104] J.-H. Kim, F. Nunio, F. Pierron, P. Vedrine, *Superconduct. Sci. Technol.* **2011**, *24*, 125001.
[105] E. M. C. Jones, J. D. Carroll, K. N. Karlson, S. L. B. Kramer, R. B. Lehoucq, P. L. Reu, D. Z. Turner, *Comput. Mater. Sci.* **2018**, *152*, 268.
[106] M. Grédiac, F. Pierron, *Int. J. Numer. Methods Eng.* **1998**, *41*, 293.
[107] M. Grédiac, F. Pierron, S. urrel Y., *Exper. Mech.* **1999**, *39*, 142.
[108] N. Souto, S. Thuillier, A. G. Andrade-Campos, *Int. J. Mech. Sci.* **2015**, *101–102*, 252.
[109] N. Souto, A. G. Andrade-Campos, S. Thuillier, *Int. J. Mater. Forming* **2017**, *10*, 353.
[110] J. Aquino, A. G. Andrade-Campos, A. Gil, J. M. P. Martins, S. Thuillier, *Strain* **2019**, *55*, e12313.
[111] J. M. P. Martins, S. Thuillier, A. G. Andrade-Campos. In: Baldi A., Kramer S., Pierron F., Considine J., S. Bossuyt, J. Hoefnagels, eds. *Residual Stress, Thermomechanics & Infrared Imaging and Inverse Problems*, Conference Proceedings of the Society for Experimental Mechanics Series, vol. 6: Springer, Cham; **2020**:25–32.
[112] F. Barlat, H. Aretz, J. W. Yoon, M. E. Karabin, J. C. Brem, R. E. Dick, *Int. J. Plasticity* **2005**, *21*, 1009.
[113] F. Almeida, B. Barroqueiro, J. Dias-de Oliveira, A. G. Andrade-Campos, *Proc. Manuf.* **2020**, *47*, 816.
[114] B. Barroqueiro, A. G. Andrade-Campos, J. Dias-de Oliveira, R. A. F. Valente, *Int. J. Mech. Sci.* **2020**, *181*, 105764.
[115] L. L. Magorou, F. Bos, F. Rouger, *Composites Sci. Technol.* **2002**, *62*, 591.
[116] M. Bertin, F. Hild, S. Roux, *Strain* **2016**, *52*, 307.
[117] L. Chamoin, C. Jailin, M. Diaz, L. Quesada, *Int. J. Solids Struct.* **2020**, *193–194*, 270.
[118] S. Avril, M. Grédiac, F. Pierron, *Comput. Mech.* **2004**, *34*, 439.
[119] F. Pierron, G. Vert, R. Burguete, S. Avril, R. Rotinat, M. R. Wisnom, *Strain* **2007**, *43*, 250.
[120] M. Rossi, P. Lava, F. Pierron, D. Debruyne, M. Sasso, *Strain* **2015**, *51*, 206.
[121] P. Wang, F. Pierron, O. T. Thomsen, *Exper. Mech.* **2013**, *53*, 1001.
[122] K. S. yed Muhammad, E. Toussaint, M. Grédiac, S. Avril, J. H. Kim, *Composite Struct.* **2008**, *85*, 70.
[123] K. Syed-Muhammad, E. Toussaint, M. Grédiac, *Struct. Multidiscipl. Optim.* **2009**, *38*, 71.
[124] S. Zhang, T. Xing, H. Zhu, X. Chen, *Materials* **2020**, *13*, 674.
[125] M. Grédiac, F. Sur, B. Blaysat, *Opt. Lasers Eng.* **2020**, *127*, 105984.
[126] F. Sur, M. Grédiac, *J. Math. Imag. Vision* **2016**, *56*, 472.
[127] H. W. Schreier, M. A. Sutton, *Exper. Mech.* **2002**, *42*, 303.
[128] F. Sur, B. Blaysat, M. Grédiac, *J. Math. Imag. Vision* **2020**. Submitted.

[129] F. Sur, M. Grédiac, *Inverse Probl. Imaging* **2014**, *8*, 259.
[130] M. Rossi, F. Pierron, *Int. J. Solids Struct.* **2012**, *49*, 420.
[131] M. Grédiac, B. Blaysat, F. Sur, *Exper. Mech.* **2017**, *57*, 871.
[132] L. Fletcher, F. Pierron, *J. Dyn. Behav. Mater.* **2018**, *4*, 481.
[133] P. Bouda, B. Langrand, D. Notta-Cuvier, E. Markiewicz, F. Pierron, *Comput. Mech.* **2019**, *64*, 1639.
[134] M. Rossi, M. Badaloni, P. Lava, D. Debruyne, F. Pierron, *AIP Conf. Proc.* **2016**, *1769*, 200016.
[135] X. Gu, F. Pierron, *Composites Part A: Appl. Sci. Manuf.* **2016**, *91*, 448.
[136] H. W. Schreier, M. A. Sutton, *Exper. Mech.* **2002**, *42*, 303.
[137] B. Blaysat, J. Neggers, M. Grédiac, F. Sur, *Exper. Mech.* **2020**, *60*, 393.
[138] X. Gu, F. Pierron, Full optimization of the T-shaped tensile test using genetic algorithm, **2016**. http://www.camfit.fr/documents/Progress_report_Xuesen_Tshape.pdf.
[139] W. Tong, *Strain* **2005**, *41*, 167.
[140] M. Dalémat, M. Coret, A. Leygue, E. Verron, *Mech. Mater.* **2019**, *136*, 103087.
[141] A. Leygue, M. Coret, J. Réthoré, L. Stainier, E. Verron, *Comput. Methods Appl. Mech. Eng.* **2018**, *331*, 184.
[142] A. Leygue, R. Seghir, J. Réthoré, M. Coret, E. Verron, L. Stainier, *Comput. Mech.* **2019**, *64*, 501.
[143] J. Réthoré, A. Leygue, M. Coret, L. Stainier, E. Verron, *Int. J. Numer. Methods Eng.* **2018**, *113*, 1810.

How to cite this article: Pierron F, Grédiac M. Towards Material Testing 2.0. A review of test design for identification of constitutive parameters from full-field measurements. *Strain*. 2020;e12370. https://doi.org/10.1111/str.12370